Two-Dimensional Surface-Enhanced Raman Imaging of a Roughened Silver Electrode Surface with Adsorbed Pyridine and Comparison with AFM Images

ARTICLE *in* THE JOURNAL OF PHYSICAL CHEMISTRY B · MAY 1996

Impact Factor: 3.3 · DOI: 10.1021/jp960048s

5 AUTHORS, INCLUDING:

Katsuhiro Ajito
Nippon Telegraph and Telephone
124 PUBLICATIONS **1,555** CITATIONS
SEE PROFILE

Donald A. Tryk
University of Yamanashi
250 PUBLICATIONS **15,556** CITATIONS
SEE PROFILE

Kenkichi Hashimoto
Kyushu Medical Center
499 PUBLICATIONS **14,525** CITATIONS
SEE PROFILE

The Journal of Physical Chemistry

 VOLUME 100, NUMBER 18, MAY 2, 1996

LETTERS

Two-Dimensional Surface-Enhanced Raman Imaging of a Roughened Silver Electrode Surface with Adsorbed Pyridine and Comparison with AFM Images

X. M. Yang, K. Ajito,† D. A. Tryk, K. Hashimoto, and A. Fujishima*

Department of Applied Chemistry, Faculty of Engineering, The University of Tokyo, 7-3-1 Hongo, Bunkyo-ku, Tokyo 113, Japan

Received: January 2, 1996[⊗]

Raman scattered light from pyridine adsorbed on an electrochemically roughened silver electrode surface was used to image the two-dimensional surface morphology with a spatial resolution of 1 μm. The images showed that the spatial distribution and intensity of the surface-enhanced Raman scattered (SERS) light intensity varied to a significant extent over the electrode surface and revealed apparent surface features, specifically, ridges and domes with dimensions on the order of 10 μm. Atomic force microscopic images also showed similar structures. In addtion, the AFM images showed that smaller surface features, on the order of 1−3 μm, were associated with brighter areas in the SERS images. However, the difference in SERS intensities for bright vs dark areas was at most a factor of ∼6, indicating that, even in the dark areas, there was significant surface enhancement. Consistent with this result is the fact that, at still higher magnification, the AFM images in different areas of the electrode showed very similar surface structure, consisting of silver particles with diameters in the range 50−400 nm.

Introduction

Following the first report of a Raman spectrum on a roughened silver surface by Fleischmann et al. in 1974[1] and the recognition of the surface-enhanced Raman scattering (SERS) effect in 1977 by Albrecht and Creighton[2] and by Jeanmaire and Van Duyne,[3] a large number of experimental studies have been carried out to obtain in situ vibrational information on electrode−electrolyte interfaces using the SERS technique.[4−7] A significant part of the work in this area has been devoted to the examination of relationships between the characteristics of the substrate metal, including the type of metal and particle size, and the characteristics of the Raman spectra, including peak intensities and positions. For example, it has been shown that SERS spectra can be obtained on silver surfaces that are either smooth, i.e., either polished polycrystalline or single crystal,[8−10] or have been subjected to only minimal roughening.[11−13] The use of colloidal silver particles of various sizes has also been examined.[14−16] A number of studies have made use of scanning electron microscopy (SEM) to examine relationships between surface morphology and SERS.[17−24] Recently scanning probe microscopy (SPM) has been used to examine substrate surfaces used for SERS, including work in our laboratory using scanning tunneling microscopy (STM)[13] and the work of Van Duyne et al. with atomic force microscopy (AFM).[25] The latter paper has shown that although significant SERS enhancement factors ($\leq 10^5$) can be associated with roughness on the scale of tens of nanometers, there can be additional enhancements ($\leq 10^2$) due to surface structures on the scale of just below 1 μm, which were obtained by depositing silver films over polymer nanospheres.

Another approach to examining the relationships between

† Present address: NTT Basic Research Laboratories, Nippon Telegraph and Telephone Corp., 3-1 Morinosato Wakamiya, Atsugi, Kanagawa 243-01, Japan.

* To whom correspondence should be addressed.

[⊗] Abstract published in *Advance ACS Abstracts,* April 15, 1996.

S0022-3654(96)00048-2 CCC: $12.00

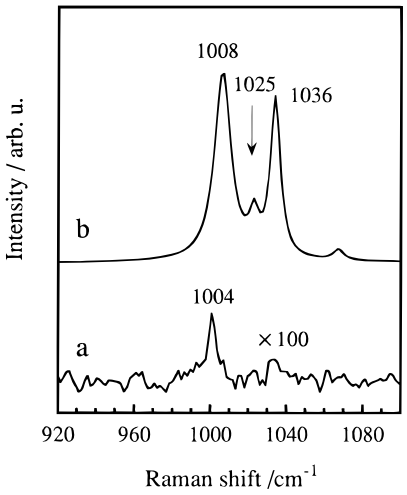

Figure 1. SERS spectra for pyridine adsorbed on silver (a) before and (b) after ORC treatment. Curves (a) and (b) were obtained with exposure times of 20 and 0.5 s, respectively.

surface microstructure and SERS signal intensity is to employ Raman imaging techniques in order to construct two-dimensional SERS images. In this letter, we present a SERS image, obtained in this way, of an electrochemically roughened silver surface with adsorbed pyridine with a spatial resolution of 1 μm. For comparison, AFM was also used to examine the electrode surface morphology on both the micrometer scale and the nanometer scale. Our results show that features in the SERS image are related to surface roughness features seen in the AFM images. To our knowledge, this is the first reported comparison of a SERS-based Raman image with AFM. In addition to reports by McGlashen et al.[26] and by Evans et al.,[27] the present work is also one of the first to describe the use of SERS as an imaging tool. This technique may also have a number of possible applications for the imaging of surface structure in which the signal intensities are insufficient for conventional Raman imaging.

Experimental Section

The silver electrode was freshly prepared by vacuum evaporation of silver onto ITO glass using a Model EX-200 evaporator (Ulvac, Inc., Japan) with an initial pressure of 4×10^{-6} Torr. The evaporation rate was approximately 2.0 Å s^{-1}, and the thickness was 0.8−1.0 μm. The electrochemical treatment was performed in a cell that was provided with the AFM system (see below). The silver electrode was roughened using an oxidation−reduction cycle (ORC) procedure for 20 min at 50 mV s^{-1} between −1.5 and 1.5 V (cell potential) in a two-electrode arrangement. From the cyclic voltammogram, the charge density for the silver-oxidation part of the cycle was 19 mC cm^{-1}, corresponding to approximately 80 monolayers of silver. The supporting electrolyte was 0.1 M KCl dissolved in

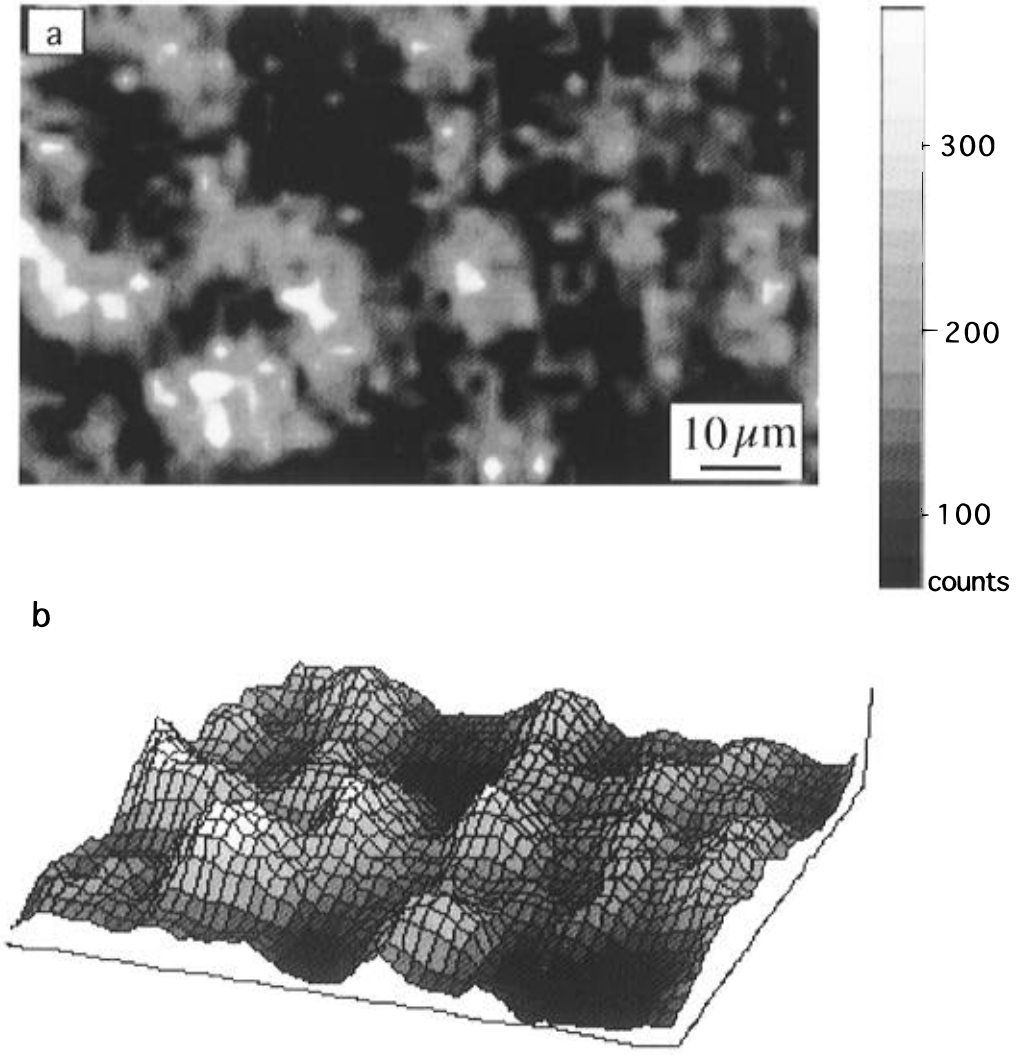

Figure 2. SERS image for pyridine adsorbed on Ag electrode over a region of 60 μm × 100 μm obtained at 1008 ± 5 cm^{-1}. Images (a) and (b) are 2D and 3D representations, respectively, of the same area.

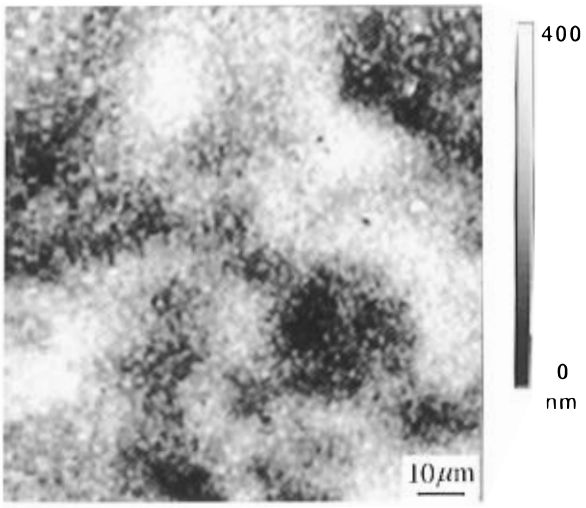

Figure 3. Low-resolution AFM image (100 μm × 100 μm) for the same electrode surface as in Figure 2.

triply distilled water, and the pyridine concentration was 0.05 M. All of the chemicals were reagent grade. Pt wire was used as the counter electrode.

The SERS spectra and images were recorded with a Renishaw imaging microscope system (Renishaw Company, UK), which has been described earlier.[28] This system has high optical throughput compared to conventional Raman systems and thus permits the use of relatively low laser power, which reduces the likelihood of sample damage. The system also has the capability of obtaining spectra relatively quickly (see below), facilitating the acquisition of Raman images which are constructed therefrom. The 514.5 nm line of an Ar^+ laser was used as the SERS excitation source. The laser light was focused onto the sample using a 50× objective lens mounted on an Olympus BH-2 microscope. The SERS imaging was performed with 5 mW excitation. The laser spot was approximately 1 μm in diameter. The sample was placed below the objective lens on an *XYZ* stage (Newport M-462-XYZ-M) equipped with stepper motors (Newport 850B), which were controlled with a motion controller (Newport PMC400). The sample surface was scanned sequentially in 1 μm steps, and full spectra (600−1430 cm^{-1}) were obtained in 0.5 s at each point. Integrated Raman intensity values at each point (i.e., pixel) for the 2D SERS image were obtained by integrating the intensities over a 5 cm^{-1} range on either side of the Raman peak for pyridine at 1008 cm^{-1}. All of the SERS images were background-corrected by subtracting a background image obtained in an off-peak portion of the Raman spectrum (955−965 cm^{-1}). The data were analyzed using software developed in-house.[29]

AFM measurements was performed in contact mode with a Seiko SPA-300 system equipped with an electrochemical cell. A triangular cantilever with integral pyramidal Si_3N_4 tip was used. The typical imaging force was on the order of 10^{-9} N.

Results and Discussion

Figure 1 shows a typical SERS spectrum for pyridine adsorbed on the silver electrode acquired on open circuit (ca. 0.04 V vs SCE). Curves a and b in Figure 1 represent the Raman spectra before and after ORC treatment, respectively. The acquisition times for Figure 1a,b were 20 and 0.5 s, respectively. The spectral acquisition time of 0.5 s was also the time used for the SERS imaging, and it can be seen that the S/N ratio was excellent due to the high sensitivity of the system. Before ORC treatment, only a very weak band at 1004 cm^{-1} was observed. After ORC treatment there was the expected large increase in Raman intensity. The two strong bands at 1008 and 1036 cm^{-1} correspond to the two symmetric ring-breathing modes of pyridine. Since these two bands are similar in frequency to those for pyridine dissolved in water, they are ascribed to pyridine physisorbed at the electrode−electrolyte interface. The relatively weak band at 1025 cm^{-1} is ascribed to pyridine chemisorbed on silver via Lewis acid coordination through the nitrogen lone pairs.[1]

Figure 2 shows the SERS image obtained for the pyridine-covered silver electrode surface. The scanning area was 60 μm × 100 μm. The brighter regions in the SERS image correspond to regions of higher SERS intensity. The SERS intensity varies to a relatively large extent over the electrode surface, allowing surface features to be observed. These take the form of circular areas from 5 to 20 μm in diameter, which are in some cases interconnected. These structures can be seen more clearly from the 3D representation of the SERS surface (Figure 2b). To

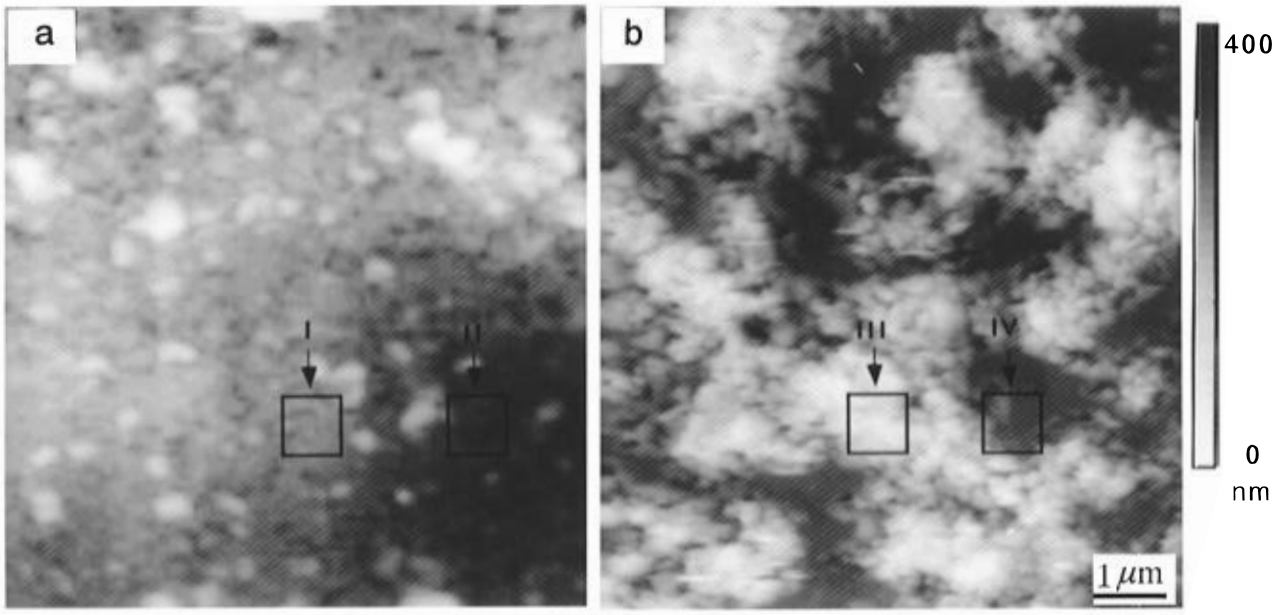

Figure 4. Medium-resolution AFM images (8 μm × 8 μm) obtained for (a) "dark" and (b) "bright" regions on the electrode surface according to Figures 2 and 3.

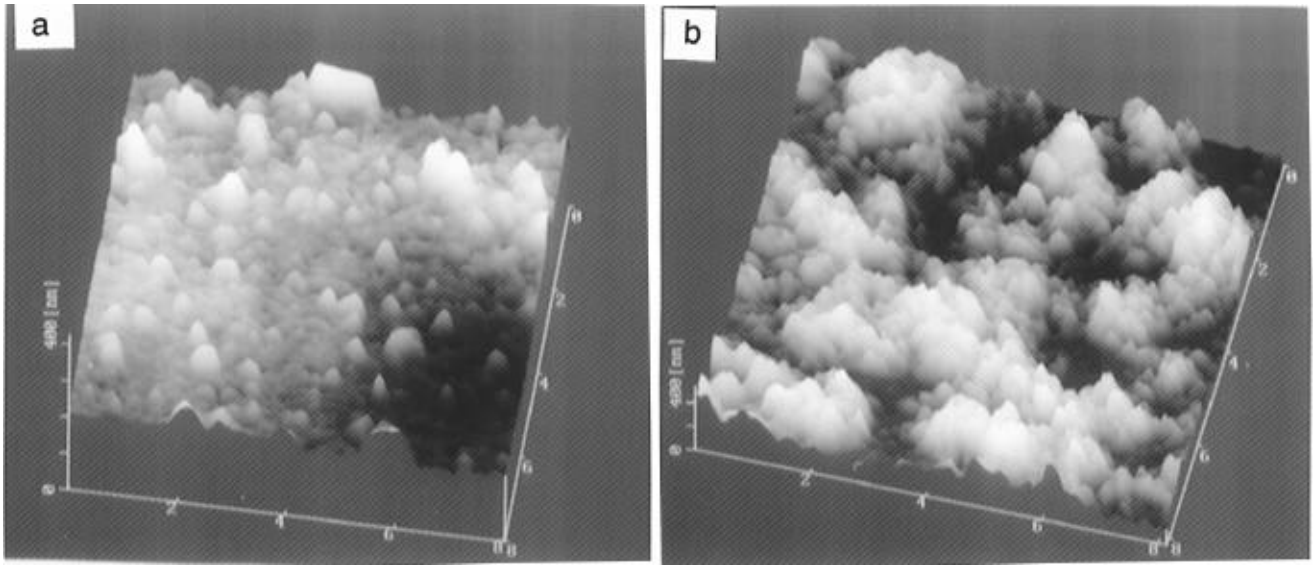

Figure 5. 3D representation of the same areas shown in Figure 4.

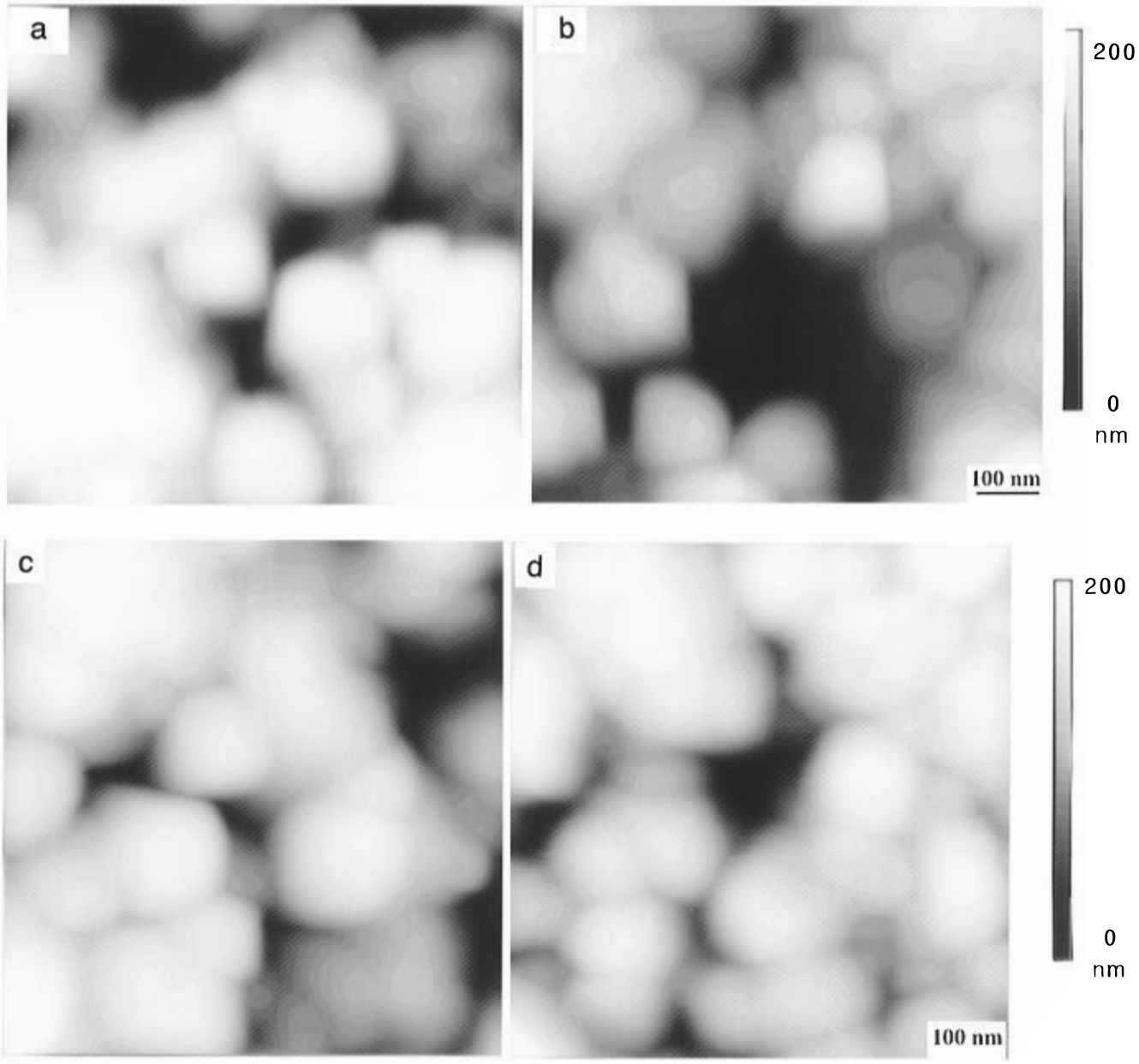

Figure 6. Higher resolution AFM images (800 nm × 800 nm) corresponding to the small square outlines in Figure 4, with (a) and (b) taken from Figure 4a (I and II, respectively) and (c) and (d) taken from Figure 4b (III and IV, respectively).

better understand this observed SERS-related structure, we characterized the electrode surface using AFM. Figure 3 shows an AFM image acquired from the same electrode surface on the same scale as the SERS image over a 100 μm × 100 μm area. Interestingly, the electrode surface also exhibited features on the order of a few μm. Here again there appear to be circular areas 10−20 μm in diameter which are somewhat interconnected. It should be stressed that, although the scanned areas for the SERS image (Figure 2) and the AFM image (Figure 3) were not identical, we have confirmed by examining other areas that the structures observed in both the SERS and AFM images are representative of the electrode surface. The similarity of the structures observed with SERS and AFM was also checked using optical microscopy.

More detailed information on the surface structure can also be obtained with AFM. Figure 4 shows two medium-resolution AFM images over a 8 μm × 8 μm area, one (Figure 4a) from a darker area of the type seen in the lower-resolution AFM image in Figure 3, and the other (Figure 4b) from a brighter area. The morphologies of the two regions show significant differences in surface roughness. The surface of the "dark" region (Figure 4a) was relatively flat, with a few dispersed particles smaller than 1 μm, whereas that of the "bright" region (Figure 4b) was relatively rough, with many features on the order of 1−3 μm. These features were typical of the "bright" regions. The difference in morphology can be seen more clearly from the 3D representation of the same two areas, as shown in Figure 5.

The surface structure was also examined on the submicrometer scale. Figure 6 shows AFM images of "dark" vs "bright" regions over an 800 nm × 800 nm area. Figure 6a,b correspond to the small square outlines in Figure 4a (I and II, respectively), whereas Figure 6c,d were taken from Figure 4b (III and IV, respectively). All of these higher resolution images were similar in appearance, consisting of spherical particles 50−400 nm in diameter. Particles in this size range have also been observed previously for electrochemically roughened surfaces by various workers with SEM.[17−19,21]

Although there is perhaps still a lack of consensus concerning the phenomena responsible for the SERS effect, there is some agreement that a significant portion of the effect is related to the presence of surface plasmons and that these are associated with roughness features below 1 μm.[18] AFM images presented here on a few hundred-nanometer scale revealed that the dimensions of the individual particles on the electrode surface were in the range 50−400 nm, so that the surface plasmon-type Raman enhancement effect should also have been similar over the whole electrode surface. At first glance, this result appears to be inconsistent with the fact that bright and dark areas were observed in the Raman image. However, although there was a significant difference in Raman intensity between bright vs dark areas, this difference was only a factor of ∼6, so that even the dark areas showed considerable enhancement, as seen in the scale in Figure 2.

These results are somewhat parallel to those of Van Duyne et al.,[25] who showed that for a surface prepared by depositing silver on a close-packed bed of 542-nm polystyrene nanospheres, the overall surface enhancement factor (10^7) could be partitioned into a major portion (10^5) due to "random substructure roughness" (RSR), with silver particles in the 30−60 nm range, and an additional, smaller factor (10^2) due to the larger-scale structure (∼500 nm) provided by the nanospheres. The latter was ascribed to surface plasmon polaritons arising from the long-range, regular undulations of the surface. This type of effect would seem to be unlikely, however, for the type of surface examined in the present work, in which the surface features observed on the order of 1−3 μm were not present in an ordered array. It may be possible that the effect that we are observing is due to a simple surface area effect, in which the SERS intensity is dependent upon the number of pyridine molecules per unit geometric surface area (as probed by the laser spot) rather than true surface area. More detailed work is needed in order to make definitive statements concerning the relationships between surface structure and SERS enhancement. Higher resolution SERS imaging particularly is needed. The present results, however, have demonstrated the potentialities of SERS as an imaging tool for a heterogeneous surface.

Acknowledgment. The authors would like to thank Mr. H. Hagiwara for his experimental assistance. This research work was partially supported by a Grant-in-Aid for Scientific Research from the Ministry of Education, Science and Culture of Japan.

References and Notes

(1) Fleischmann, M.; Hendra, P. J.; McQuillan, A. J. *Chem. Phys. Lett*. **1974**, *26*, 163.
(2) Albrecht, M. G.; Creighton, J. A. *J. Am. Chem. Soc*. **1977**, *99*, 5215.
(3) Jeanmaire, D. L.; Van Duyne, R. P. *J. Electroanal. Chem.* **1977**, *84*, 1.
(4) Chang, P. K., Furtak, T. E., Eds. *Surface Enhanced Raman Scattering*; Plenum Press: New York, 1982.
(5) Moskovits, M. *Rev. Mod. Phys*. **1985**, *57*, 783.
(6) Metiu, H.; Das, P. *Annu. Rev. Phys. Chem.* **1984**, *35*, 507.
(7) Campion, A. *Annu. Rev. Phys. Chem*. **1985**, *36*, 549.
(8) Schultz, S. G.; Janik-Czachor, M.; Van Duyne. R. P. *Surf. Sci.* **1981**, *104*, 419.
(9) Tsang, J. C.; Avouris, P.; Kirtley, J. R. *J. Electron Spectrosc. Relat. Phenom.* **1983**, *29*, 343.
(10) Sueoka, T.; Inukai, J.; Ito, M. *J. Electron Spectrosc. Relat. Phenom.* **1993**, *64/65*, 363.
(11) Pettinger, B.; Wenning, U. *Chem. Phys. Lett*. **1978**, *56*, 253.
(12) Pettinger, B.; Wenning, U.; Wetzel, H. *Chem. Phys. Lett*. **1979**, *67*, 192.
(13) Sakamaki, K.; Itoh, K.; Hashimoto, K.; Fujishima, A. *J. Vac. Sci. Technol*. **1990**, *A8*, 525.
(14) Creighton, J. A. In *Surface Enhanced Raman Scattering*; Chang, P. K., Furtak, T. E., Eds.; Plenum Press: New York, 1982; p 315.
(15) Montes, R.; Contreras, C.; Ruperez, A.; Laserna, J. J. *Anal. Chem.* **1992**, *64*, 2715.
(16) Freeman, R. G.; Grabar, K. C.; Allison, K. J.; Bright, R. M.; Davis, J. A.; Guthrie, A. P.; Hommer, M. B.; Jackson, M. A.; Smith, P. C.; Walter, D. G.; Natan, M. J. *Science* **1995**, *267*, 1629.
(17) Evans, J. F.; Albrecht, M. G.; Ullevig, D. M.; Hexter, R. M. *J. Electroanal. Chem.* **1980**, *106*, 209.
(18) Schultz, S. G.; Janik-Czachor, M.; Van Duyne, R. P. *Surf. Sci.* **1981**, *104*, 419.
(19) Busby, C. C.; Creighton, J. A. *J. Electroanal. Chem.* **1982**, *140*, 379.
(20) Murphy, D. V.; Von Raben, K. U.; Chen, T. T.; Owen, J. F.; Chang, R. K. *Surf. Sci.* **1983**, *124*, 529.
(21) Devine, T. M.; Furtak, T. E.; Macomber, S. H. *J. Electroanal. Chem.* **1984**, *164*, 299.
(22) Pemberton, J. E.; Girand, M. M. *J. Electroanal. Chem.* **1987**, *217*, 79.
(23) Cross, N. A.; Pemberton, J. E. *J. Electroanal. Chem.* **1987**, *217*, 93.
(24) Pemberton, J. E.; Guy, A. L.; Sobocinski, R. L.; Tuschel, D. D.; Cross, N. A. *Appl. Surf. Sci.* **1988**, *32*, 33.
(25) Van Duyne, R. P.; Hulteen, J. C.; Treichel, D. A. *J. Chem. Phys*. **1993**, *99*, 2101.
(26) McGlashen, M. L.; Guhathakurta, U.; Davis, K. L.; Morris, M. D. *Appl. Spectrosc.* **1991**, *45*, 543.
(27) Evans, S. D.; Freeman, T. L.; Flynn, T. M.; Batchelder, D. N.; Ulman, A. *Thin Solid Films* **1994**, *244*, 778.
(28) Ajito, K.; Sukamto, J. P. H.; Nagahara, L. A.; Hashimoto, K.; Fujishima, A. *J. Electroanal. Chem.* **1995**, *386*, 229.
(29) Ajito, K.; Sukamto, J. P. H.; Nagahara, L. A.; Hashimoto, K.; Fujishima, A. *J. Vac. Sci. Technol*. **1995**, *A13*, 1234.

JP960048S